Rap1, Canoe and Mbt cooperate with Bazooka to promote *zonula adherens* assembly in the fly photoreceptor

Rhian F. Walther[1], Mubarik Burki[1,2], Noelia Pinal[1,3], Clare Rogerson[1] and Franck Pichaud[1]*

[1] MRC Laboratory for Molecular Cell Biology, University College London, Gower Street, London, WC1E 6BT, United Kingdom.

[2] Current address: Randall Division of Cell and Molecular Biophysics, Kings College London, London, SE1 1UL, United Kingdom.

[3] Current address: Centro de Biología Molecular, CSIC-UAM, Madrid, Spain.

*Corresponding author: f.pichaud@ucl.ac.uk

Phone: (+44) 0 207 679 7817

Fax: (+44) 0 207 679 7805

Abstract

In *Drosophila* epithelial cells, apical exclusion of Bazooka/Par3 defines the position of the *Zonula Adherens (ZA),* which demarcates the apical and lateral membrane and allows cells to assemble into sheets. Here, we show that the small GTPase Rap1, its effector AF6/Canoe (Cno) and the Cdc42-effector Pak4/Mushroom bodies tiny (Mbt), converge in regulating epithelial morphogenesis by coupling stabilization of the *Adherens Junction (AJ)* protein E-Cadherin, and Bazooka retention at the *ZA*. Furthermore, our results show that the localization of Rap1, Cno and Mbt at the *ZA* is interdependent, indicating their functions during *ZA* morphogenesis are interlinked. In this context, we find the Rap1-GEF Dizzy is enriched at the *ZA* and our results suggest it promotes Rap1 activity during *ZA* morphogenesis. Altogether, we propose the Dizzy, Rap1/Cno pathway and Mbt converge in regulating the interface between Bazooka and *AJ* material to promote *ZA* morphogenesis.

Introduction

The epithelial *Zonula Adherens (ZA)* enables cell-cell adhesion, allowing epithelial cells to assemble into sheets and form organs. Elucidating how *ZA* morphogenesis is regulated during epithelial cell morphogenesis remains an important goal in epithelial cell biology. The *ZA* includes the adhesion molecule E-Cadherin/Shotgun (E-Cad) and its effector βcatenin/Armadillo (Arm), which are main *Adherens Junction (AJ)* components that mediate cell-cell adhesion (Tepass, 2012). Several factors regulate *AJ* material morphogenesis and accumulation during *ZA* assembly. These include the small GTPase Rap1 and its effector actin binding protein Cno/AF6 (Bos et al., 2001; Niessen and Gottardi, 2008; Pannekoek et al., 2009), the type-2 p21-activated kinase Mushroom bodies tiny (Mbt/Pak4) (Menzel et al., 2007; Wallace et al., 2010; Walther et al., 2016), and the Par complex (Cdc42-Par6-aPKC-Bazooka) (McGill et al., 2009; Morais-de-Sa et al., 2010; Walther and Pichaud, 2010). However, we lack an integrated view of how these factors come together to regulate *ZA* morphogenesis and remodeling during epithelial cell morphogenesis.

The pupal photoreceptor has long been used as a model system to study the genetic and molecular basis for the specification and morphogenesis of the epithelial apical, sub-apical and *ZA* membrane domains. In these cells, these domains are clearly separated along the apical basal (X-Y) axis (Figure 1A-C), and the apical organelle, called the rhabdomere, is analogous to the epithelial brush border and consists of approximately 60 000 microvilli. The sub-apical membrane is called stalk and can be up to 1.5 microns in length, and connects the rhabdomere to the more basal *ZA*. These three membrane

domains are specified early during pupal development and undergo sustained morphogenesis as the cells elongate by approximately 10 fold to generate the lens (proximal) to brain (distal) axis of the retina (Ready, 2002) (Figure 1A-B). In pupal photoreceptors, the Par complex regulates the separation of the *ZA* from the stalk membrane (Hong et al., 2003; Nam and Choi, 2003; Walther et al., 2016; Walther and Pichaud, 2010). Concomitantly, the conserved transmembrane protein Crumbs (Crb) functions with the Par complex to drive stalk membrane and *ZA* morphogenesis as photoreceptors elongate along the proximal-distal axis of the retina (Izaddoost et al., 2002; Pellikka et al., 2002).

In *Drosophila* epithelia, Bazooka (Baz) phosphorylation at Serine S980 by aPKC is essential for specifying the *ZA* and sub-apical membrane. Baz phosphorylation occurs upon Par complex assembly and is thought to allow for Crb to capture Cdc42-Par6-aPKC, thus leading to the apical exclusion of P-S980-Baz (Krahn et al., 2010; Morais-de-Sa et al., 2010; Walther and Pichaud, 2010). Confined to the apical-lateral border of the cell, P-S980-Baz is then thought to promote *ZA* assembly, at least in part through its ability to bind to Arm (Wei et al., 2005). In the pupal photoreceptor, Crb/Par6-aPKC accumulate at the stalk membrane and P-S980-Baz is found immediately basal to it, at the developing *ZA* (Figure 1B-C). It is likely that Par3 phosphorylation and concomitant apical exclusion plays a similar role in vertebrate neuroepithelial cells. In vertebrates, Par3 is phosphorylated by aPKC (Nagai-Tamai et al., 2002), and in neuroepithelial cells, is found basal to aPKC/Par6, at the *Apical Junctional Complex (AJC),* which contains Cadherins (Aaku-Saraste et al., 1996; Afonso and Henrique, 2006).

Next to Baz, the P21-activated kinase Mushroom bodies tiny (Mbt) and its vertebrate homologue Pak4 have also been shown to regulate *ZA* morphogenesis. In pupal photoreceptors, Mbt regulates *ZA* morphogenesis and overall apical membrane differentiation by promoting the accumulation of the E-Cad-Arm complex via phosphorylating βCat/Arm and regulating the F-actin cytoskeleton, which in turn is essential for the retention of Baz at the *ZA* (Jin et al., 2015; Law and Sargent, 2014; Menzel et al., 2008 Schneeberger, 2003 #1892; Walther et al., 2016). In these cells, failure to retain *AJ* material, including Baz at the *ZA* leads to a shortening of the *ZA* along the apical-basal axis of the cell. In addition severe defects in polarized photoreceptor morphogenesis can occur (Walther et al., 2016). In vertebrate cells, Pak4 also regulates *ZA* maturation (Jin et al., 2015; Law and Sargent, 2014; Wallace, 2010 #2493), and its function during epithelial morphogensis has been linked to that of the Par complex, as Pak4 phosphorylates Par6b (Jin et al., 2015; Wallace et al., 2010). While in flies Mbt does not phosphorylate Par6, Mbt and Baz are main regulators of *AJ* material accumulation at the plasma membrane. In the absence of *baz, AJ* material can still be detected at the plasma membrane of pupal photoreceptors within the apical pole of the cell. Similarly, *ZA* domains are present in *mbt* null mutant cells, albeit shorter and presenting less *AJ* material than in wild type cells. However, no *AJ* domains are found in photoreceptors mutant for both *baz* and *mbt,* indicating that Baz and Mbt function in parallel pathways to promote *AJ* morphogenesis and/or stabilization at the plasma membrane (Walther et al., 2016).

Another conserved factor that regulates *AJ* material morphogenesis is Rap1, which in epithelia can be activated by the PDZ-GEF protein Dizzy (Dzy) (de Rooij et al., 1999; Kawajiri et al., 2000). Rap1 has been shown to localize at the *AJ* in various fly epithelia, and to be an essential *AJ* regulator (Boettner et al., 2003; Boettner and Van Aelst, 2007; Choi et al., 2013; Knox and Brown, 2002; O'Keefe et al., 2009; Spahn et al., 2012; Wang et al., 2013). In the fly embryo, Rap1 and its effector F-actin binding protein Cno (Boettner et al., 2003; Mandai et al., 2013; Sawyer et al., 2009), regulate the apical localization of both Baz and Arm, with Baz reciprocally influencing Cno localization. Furthermore, Baz is required to capture preassembled *AJ* material, thus promoting the morphogenesis of Spot *AJs*, which are precursors of the *ZA* in this tissue (McGill et al., 2009). In addition, work in human MCF7 cells has shown a role for Rap1 during *AJ* maturation via promoting E-Cad recruitment at the sites of cell-cell contact, a function that has been shown to be mediated, at least in part, by Cdc42 (Hogan et al., 2004). However, how the functions of Rap1, Cno, Baz and Mbt relate to each other during *ZA* morphogenesis has not been examined.

Results

Rap1 regulates pupal photoreceptor *ZA* morphogenesis

In the fly retina, Rap1 has been previously shown to regulate *AJ* remodeling between newly specified photoreceptors, and between retinal accessory cells that surround the photoreceptors (cone and pigment cells) (O'Keefe et al., 2009). To examine the distribution of Rap1 and its GEF Dzy in the pupal

photoreceptor (Figure 1A-C), we made use of the *rap1-Rap1::GFP* and *dzy-Dzy::GFP* transgenes, which allow for expression of these proteins under the control of their endogenous promoter. We found that Rap1::GFP is present at the apical membrane and accumulates predominantly at the developing *ZA* (Figure 1D-F). Dzy::GFP (Figure 1G) shows a low level expression all over the apical membrane and presents a slight but reproducible enrichment at the developing *ZA* (Figure 1G-H). These results suggest that Dzy/Rap1 might regulate apical membrane and *ZA* morphogenesis in the pupal photoreceptor.

To assess the function of Rap1 during photoreceptor morphogenesis, we made us of available *Rap1* loss-of-function alleles. We found that generating mutant clones using the strong allele *Rap1CD3*, or expressing high levels of a previously validated *Rap1IR* (Rap1 RNAi) construct (O'Keefe, 2009 #1401), leads to severe defects in recruiting the full complement of retinal accessory cells including the cone cells (Supplementary Figure 1A). Missing cone and pigment cells lead to retinal cell delamination, with many photoreceptors found below the floor of the retina (Supplementary Figure 1B-D), preventing us from assessing polarity and *ZA* morphogenesis. In order to bypass this strong phenotype we limited the expression of *Rap1IR*. Decreasing the expression of *Rap1* at pupal stages did not affect photoreceptor apical-basal polarity in the majority of ommatidia examined (Figure 2A-C). However, quantification revealed the length of the Arm, Mbt and Baz domains, measured along the apical-basal axis, was significantly reduced when compared to wild type (Figure 2D-D''). In addition, while the levels of Arm and Baz were comparable to that measured in wild type cells (Figure 2E, 2E''), we

found Cno accumulation at the *ZA* was nearly abolished (Figure 2A'', 2D''' and 2E''') and Mbt levels were significantly decreased when compared to wild type (Figure 2B'' and 2E'). We also note that apical levels of F-actin (Figure 2A'''), aPKC (Figure 1B'''), and Crb (Figure 2C'''), were not affected in *Rap1IR* photoreceptors when compared to wild type. These data indicate that Rap1 is required for the accumulation or retention of Cno and Mbt at the developing *ZA* and for regulating the length of the *ZA* along the apical-basal axis.

Rap1 promotes E-Cadherin stabilization at the *ZA*

We have previously shown that in pupal photoreceptors, loss of *mbt* function leads to an increase in the mobile fraction of E-Cad at the *ZA* when compared to wild type over 250 seconds (Walther et al., 2016). Our analysis of *Rap1IR* indicates that Mbt accumulation is strongly reduced at the *ZA* (Figure 2B'' and 2E'), which should therefore be accompanied by an increase in E-Cad mobility. To assess whether this is the case, we made use of FRAP and compared the recovery after photo-bleaching of a *ubi-ECad::GFP* transgene in wild type and *Rap1IR* photoreceptors. In wild type cells, over approximately 250 sec, we estimated that 25% of E-Cad::GFP is mobile, which is consistent with previous estimations from our lab (Walther et al., 2016) (not shown). However, while E-Cad::GFP shows a stronger recovery over this relatively short time scale in *Rap1IR* when compared to wild type, the GFP signal failed to plateau (not shown), preventing us from extrapolating the mobile fraction. We therefore performed FRAP over a longer time scale (1000 sec). Over this long time scale, we found approximately 35% of E-Cad::GFP is mobile in wild type *ZA*, while ~70% is mobile in *Rap1IR* photoreceptors (Figure 2F-G).

These data indicate that Rap1 promotes E-Cad stabilization at the *ZA,* and are compatible with Mbt mediating part of Rap1 function during this process.

Dzy regulates *ZA* morphogenesis through Rap1

To examine the function of the Rap1-GEF *dzy* during photoreceptor morphogenesis we made use of the strong *dzy*$^{\Delta\ 12}$ allele. We found that reducing *dzy* expression leads to a phenotype similar to that seen in the hypomorphic *Rap1IR* photoreceptors (Figure 3A), including a notable decrease the length of the Arm, (Figure 3A' 3B', 3C', 3D' and 3E), Mbt (Figure 3A'', 3B'', 3D'' and 3E'), Cno (Figure 3A''', 3B''' and 3E'') and Baz (Figure 3D''' and 3E''') domains along the apical basal axis of the cell. In addition, the levels of Arm, Mbt and Cno are significantly reduced at the *ZA* when compared to wild type cells (Figure 3F-F''), but those of Baz were similar to that measured in wild type cells (Figure 3F'''). Consistent with Dzy acting as a Rap1-GEF in photoreceptors, removing a copy of the *dzy* locus enhances the mild rough-eye phenotype obtained when reducing the expression of *Rap1IR* (Supplementary Figure 2). However, we note that the *dzy* loss-of-function phenotype is much milder than that of *Rap1*^{CD3} and strong *Rap1IR* in that no cells delaminate below the floor of the retina in *dzy* mutant clones. Other Rap1-GEFs must therefore be at play in the developing retina.

Cno couples Arm and Baz at the *ZA* and is required for the apical accumulation of aPKC and Crb

Next to regulating Mbt accumulation at the *ZA*, one likely mechanism whereby Rap1 might promote E-Cad stabilization is through the F-actin linker Cno. In the pupal photoreceptor, Cno is enriched at the *ZA* and found at low levels at the apical membrane in manner that is similar to the Arm expression pattern (Figure 2A'' and 2D'''). To assess Cno function we made use of the strong *cno^{R2}* allele. We found that *cno^{R2}* mutant photoreceptors delaminate through the floor of the retina (Figure 4A-B), a phenotype resembling that obtained when strongly reducing *Rap1* expression. As for the *Rap1^{CD3}*, polarity of the delaminated photoreceptors is strongly compromised in *cno^{R2}* mutant cells and the delamination phenotype is likely due defects in assembling the full complement of interommatidial accessory cells. In order to circumvent the delamination phenotype, we made use of *cnoIR* (*cno RNAi*). Examining retinas mosaic for *cnoIR* revealed that Cno regulates the length of the *ZA* and is required for the accumulation of Arm (Figure 4C', 4E' and 4G, 4H), Baz (Figure 4C'' and 4H') and Mbt (Figure 4E'', 4G'' and 4H'') at the developing *ZA*. We also noted instances where Arm was present at the *ZA* but Mbt was absent (Figure 4D and 4F). The similarity between the *Rap1IR* and *cnoIR ZA* phenotypes suggests that Rap1 and Cno function during *ZA* morphogenesis are linked. However, in the case of *cnoIR*, we also detect *ZAs* without Baz, a phenotype not detected in *Rap1IR* and indicative of a failure in retaining Baz at the developing *ZA*. Lack of Baz at the *ZA* is seen when overexpressing a

version of Arm that cannot be phosphorylated by Mbt (ArmSA^{mbt}) raising the possibility Mbt mediates Cno function (Walther et al., 2016). To test this possibility we expressed a phospho-mimetic version of Arm (ArmSE^{mbt}) in *cnoIR* retinas. However, this did not ameliorate the *cnoIR* phenotype when considering *ZA* length along the apical-basal axis and Baz retention at the *ZA* (Supplementary Figure 3).

In addition, we observed that unlike for *Rap1IR*, levels of Crb and aPKC were decreased in *cnoIR* mutant cells (Figure 4C''' and 4E'''), indicating that Cno might regulate the accumulation of these factors during apical membrane morphogenesis. However, we note that our manipulation of Rap1 levels using *Rap1IR* does not lead to a complete loss of Cno at the *ZA* (Figure 2A'' and 2E'''), while Cno is virtually undetectable in our *cnoIR* experiments (Supplementary Figure 4). We therefore envisage that residual Cno in *Rap1IR* is sufficient to support the retention of Baz at the *ZA* and the apical accumulation of Crb and aPKC.

Mbt is required for the accumulation of Cno and enrichment of Rap1 at the *ZA*

Our results indicate that Rap1 is required for the recruitment of Cno and Mbt at the photoreceptor *ZA.* Compatible with Cno mediating Rap1 function in promoting Mbt accumulation at the *ZA*, Mbt is strongly decreased in *cnoIR* photoreceptors (Figure 4E'' and 4H''). Conversely, we find that Cno accumulation at the *ZA* depends on *mbt* (Figure 5A-A''). Therefore the localization of Cno and Mbt at the *ZA* are interlinked. To examine the

functional relationship between Rap1, Cno and Mbt, and to test whether Cno and Mbt mediate Rap1 function during *ZA* morphogenesis, we asked whether expressing Mbt or Cno could ameliorate the *Rap1IR ZA* phenotype. We found that despite expressing high levels of *mbt* (Supplementary Figure 5), the *Rap1IR* phenotype was not ameliorated (Figure 5B and 5D). Similarly, expressing *cno* in *Rap1IR* cells did not restore Mbt accumulation to wild type and did not ameliorate the length of the *ZA* and (Figure 5C and 5D).

Next, we assessed whether *Rap1* could mediate part of *mbt* function by expressing the *rap1-Rap1::GFP* transgene in *mbt*[P1] null mutant cells. *mbt*[P1] mutant cells are characterized by a decreased accumulation of Arm, Baz (Walther et al., 2016) (Supplementary Figure 6A-B), and Cno (Figure 5A'') at their *ZA*. When expressing *rap1-Rap1::GFP* in *mbt*[P1] mutant cells (Figure 5E-G), we did not measure any significant recovery in the length of the Arm (Figure 5F', 5G' and 5H) or Baz domains (Figure 5E', 5H'), when compared to *mbt*[P1] mutant cells, and Cno levels were not restored (Figure 5G''). However, we noted that Rap1::GFP lacked the relative enrichment at the *ZA* normally detected in wild type cells at this developmental stage (Figure 1F and 5I-I').

One possibility is that Mbt might regulate the localization of Dzy, which in turn could shape that of Rap1. To test this possibility we examined the localization of Dzy::GFP in *mbt*[P1] mutant photoreceptors and found it is undetectable when compared to wild type (Supplementary Figure 6C-D). It is therefore possible that Mbt influences Rap1 distribution along the apical-basal axis through Dzy.

Dzy, Rap1, Cno synergize with Baz to promote *AJ* accumulation at the plasma membrane

In order to test whether the Rap1-Cno pathway mediates part of Baz function in promoting *AJ* material accumulation at the plasma membrane, we made use of genetics to probe the relationship between *Rap1* and *baz*. Firstly, we found that *Rap1* and *baz* genetically interact during eye development, as decreasing the expression of *baz* using RNAi (*bazIR*), enhances the *Rap1IR* rough eye phenotype (Supplementary Figure 2A-B, 2E-F). Secondly, to assay whether Rap1 function during *AJ* morphogenesis relates to that of Baz we generated photoreceptors deficient for both *baz* (using the *baz^{xi106}* allele) and *Rap1* (using the *NP-Gal4^{2631}-Rap1IR* strain) (O'Keefe et al., 2009). As we have shown before (Walther et al., 2016), *AJ* material such as Arm is detected at the plasma membrane in *baz^{xi106}* and *mbt^{P1}* single mutant cells (Figure 6A' and Supplementary Figure 6B'). However, no *AJ* material is detected in *baz^{xi106}, mbt^{P1}* double mutant cells (Figure 6B) indicating that *baz* and *mbt* function through parallel pathways to promote *AJ* material accumulation at the plasma membrane. We found that expressing *Rap1IR* in *baz^{xi106}* photoreceptors led to fewer cortical domains positive for Arm shared by flanking photoreceptors when compared to *baz^{xi106}* and *Rap1IR* single mutant cells (Figure 6C' and 5E). This was accompanied by a loss of Mbt (Figure 6C'''), which is consistent with our observation that Rap1 is required for the accumulation of Mbt at the *ZA* (Figure 2B'', and 2E'). In contrast, *AJ* domains containing Arm are still present in double *mbt^{P1}, Rap1IR* (Figure 6D-E). Altogether, these data argue that while the respective functions of Rap1/Cno,

Mbt and Baz converge during *ZA* morphogenesis, Rap1/Cno/Mbt function in parallel of Baz to promote *AJ* accumulation at the plasma membrane.

Discussion

In the pupal photoreceptor, *ZA* morphogenesis is orchestrated by a conserved protein network that includes Cdc42, Par6, aPKC, Baz, Crb and its binding partner Sdt, and Par1 (Berger et al., 2007; Hong et al., 2003; Izaddoost et al., 2002; Nam and Choi, 2003; Pellikka et al., 2002; Richard et al., 2006; Walther et al., 2016; Walther and Pichaud, 2010). In turn, *AJ* material is an essential part of the regulatory network that orchestrates polarity (Walther et al., 2016). We and others have previously shown that Mbt regulates pupal photoreceptor development by promoting *ZA* morphogenesis (Menzel et al., 2007; Walther et al., 2016). During this process Mbt contributes in preventing Baz from spreading to the lateral membrane, a regulation that we have found depends in part on the phosphorylation of Arm by Mbt at S561 and S688. We proposed that Mbt regulates photoreceptor polarity by promoting the retention of Baz at the developing *ZA*. Failure in *ZA* retention leads to Baz spreading to the lateral membrane where it is eliminated through Par1-mediated displacement. In these cells, failure to retain *AJ* material including Baz at the *ZA* leads to its shortening along the apical basal axis and can impact on the polarization program of the photoreceptor (Walther et al., 2016).

In the present study, we show that Mbt function is linked to that of Dzy/Rap1 and Cno. Firstly, Cno and Mbt accumulation at the *ZA* is interdependent, reflecting a tight coupling between the Rap1/Cno pathway and Mbt. Secondly, we find that Cno promotes Baz retention at the *ZA*, as *cnoIR* leads to shorter *ZA* that can be depleted of Arm and Baz. This phenotype resembles that of *mbt* mutant cells and is also seen when overexpressing a version of Arm that cannot be phosphorylated by Mbt (Walther et al., 2016). These observations prompted us to test the hypothesis that Rap1/Cno and Mbt might function as part of a linear pathway promoting Baz retention at the *ZA*. In this pathway, we reasoned that Mbt could mediate Rap1 function through Arm phosphorylation. In testing this hypothesis we found that this is not the case. Instead, the observation that expressing a version of Arm that mimics its constitutive phosphorylation by Mbt does not ameliorate the *cnoIR* phenotype suggests that Rap1/Cno and Mbt converge in promoting Baz retention at the *ZA*, and cannot compensate for each other during this process. This conclusion is well supported by the finding that overexpressing *cno* in *mbt* mutant cells does not lead to an amelioration of the *mbt* phenotype. Thirdly, we found that Mbt influences the distribution of Rap1 along the apical-basal axis of the cell in that Rap1::GFP no longer accumulates preferentially at the *ZA.* This correlates with a loss of Dzy::GFP at the plasma membrane, raising the possibility that Mbt might regulate Rap1 through Dzy. However, the *dzy* phenotype is milder than that of *Rap1* or *cno*, in that loss of *dzy* does not lead to cell delamination from the retina. This suggests that, as recently reported in

the cellularizing embryo (Bonello et al., 2018; Schmidt et al., 2018), other GEFs regulate Rap1 during epithelial morphogenesis.

An interesting aspect of the *cnoIR* phenotype is the defects in apical accumulation of aPKC and Crb. These defects are not observed in *dzy* mutant or *Rap1IR* cells, indicating that Cno might function independently of Rap1 during this process. However, we note that while we cannot detect Cno at the *ZA* of *cnoIR* cells, we still detect it in *Rap1IR* cells. We therefore hypothesize that residual Cno in *Rap1IR* cells supports optimum aPKC/Crb accumulation at the apical membrane. In our model, Dzy, Rap1 and Cno function as part of the same pathway, which includes a function in promoting optimum apical accumulation of Crb/aPKC. Baz is required for Par complex assembly and associated aPKC/Crb recruitment at photoreceptor apical membrane (Walther et al., 2016; Walther and Pichaud, 2010). We hypothesize that the defects in Crb/aPKC we detect in *cnoIR* cells are linked to the failure in retaining Baz at the *ZA* which leads to its elimination from the lateral membrane by Par1. More work will be required to understand how exactly *AJ* material and *ZA* retention of Baz influences apical membrane specification.

Rap1 and *cno* have been shown to regulate apical-basal polarity in the cellularizing embryo. In this model system, Rap1 and Cno regulate the apical localization of Baz and Arm, which precedes the apical recruitment of Crb. In turn, Baz influences the localization of Cno (Choi et al., 2013). Our work indicates that similar complex regulations are at play in the pupal photoreceptor. However, unlike in the early embryo, *AJ* material (Arm) is

absolutely required for Baz (and Par6-aPKC) accumulation/retention at the cell cortex in the developing pupal photoreceptor (Walther et al., 2016). We therefore favor a model whereby Mbt, Rap1 and Cno influence *ZA* morphogenesis primarily through regulating the interface between E-Cad/Arm, Baz and the F-actin cytoskeleton. In this model, Mbt regulates this interface both through Arm phosphorylation and cofilin dependent regulation of F-actin (Walther et al., 2016), and Cno contributes in this process at least in part through its ability to bind to F-actin.

To probe Rap1/Cno function during photoreceptor *ZA* morphogenesis, we assessed the effect of decreasing Rap1 expression on E-Cad stability. Consistent with the notion that the function of *mbt* and *Rap1* are linked during *ZA* morphogenesis, we find that, as it is the case for Mbt (Walther et al., 2016), Rap1 is required to stabilize E-Cad::GFP at the photoreceptor *ZA*. However, the mobile fraction estimated for E-Cad is much higher in *Rap1IR* cells than in *mbt^P1* null cells — evaluated at approximately 70% for *Rap1IR* and 45% for *mbt^P1* (Walther et al., 2016). Together with our finding that Mbt accumulation at the *ZA* is decreased in *Rap1IR* cells, our FRAP data are therefore compatible with Mbt mediating part of Rap1's function in promoting E-Cad stability. However, the much larger mobile fraction we estimate in the *Rap1IR* genotype when compared to *mbt^P1* photoreceptors indicates that Rap1 must also regulate E-Cad stability independently of Mbt. The longer time scale for E-Cad::GFP to recover in *Rap1IR* cells when compared to *mbt^P1* mutant cells is compatible with Rap1 functioning in part through promoting E-Cad delivery.

Acknowledgements

Material and Methods

Fly strains:

The following fly strains were used:

rap1-Rap1::GFP and *NP-Gal4²⁶³¹ , UAS-Rap1IR* (O'Keefe et al., 2009)

Rap1IR (BL #29434), *bazIR* (BL #39072), *cnoIR* (BL #33367) and *UAS-LacZ* (BL #3956).

dzy$^{\Delta 12}$, FRT40A (Huelsmann et al., 2006)

dzy-Dzy::GFP (Boettner and Van Aelst, 2007)

ubi-Cad::GFP (Oda and Tsukita, 2001)

mbt^{P1} and UAS-Mbt (Schneeberger and Raabe, 2003)

mbt^{P1}, FRT19A;, mbt^{P1}, baz^{xi106} , FRT9.2 ;, ;;UAS-ArmWT, ;;UAS-ArmSA^{mbt}

and ;;UAS-ArmSE^{mbt} *(Walther et al., 2016).*

w,baz^{xi106} , FRT9.2 (Nusslein-Volhard et al., 1987)*.*

FRT82B, cno^{R2} (Sawyer et al., 2009)

UAS-Cno (Matsuo et al., 1997)

GMR-Gal4 (Freeman, 1996)

NP-Gal4^{2631} (DGRC #104266) (Hayashi et al., 2002).

Analysis of gene function

Clonal analysis of mutant alleles in the retina was performed using the standard FLP-FRT technique (Xu and Rubin, 1993) with appropriate *FRT, ubi-GFP* chromosomes used to generate negatively marked mutant tissue in combination with eyFLP (Newsome et al., 2000). Retina expressing RNAi in clones were generated using the coinFLP system (Bosch et al., 2015). Clones of retinal tissue expressing RNAi against *Rap1* were generated both with and without UAS-dicer, while clones of retinal tissue expressing RNAi against *cno* were generated without UAS-dicer only. In order to mitigate the strong *Rap1* loss of function phenotype, *Rap1IR* animal were raised at 20 degrees and shifted to appropriate temperature (25 or 29 degrees) at puparium formation. UAS transgenes were co-expressed with UAS-*Rap1IR* or UAS-*cnoIR* under the control of the *NP-Gal4^{2631}* or *GMR-Gal4* drivers respectively.

Antibodies and immunological methods

Whole mount retinas at 40% after puparium formation (APF) were prepared as previously described (Walther and Pichaud, 2006). The following antibodies were used: rabbit anti-PKCζ, 1/600 (SAB4502380, Sigma), mouse anti-Arm, 1/200 (N27-A1, Developmental Studies Hybridoma Bank), rat anti-Baz, 1/1000 (Gift from A.Wodarz, University of Cologne), rabbit anti-Cno, 1/200 (Gift from L. Van Aelst, (Boettner et al., 2003)), rabbit anti-Baz, 1/2000, rat anti-Crb, 1/200, Guinea Pig anti-Mbt 1/200 (Walther et al., 2016), with the appropriate combination of mouse, guinea pig, rabbit and rat secondary antibodies conjugated to Dy405, Alexa488, Cy3 or Cy5 as appropriate at 1/200 each (Jackson ImmunoResearch) or TRITC-conjugated Phalloidin (P1951, Sigma) at 2μg/mL. Retinas were mounted in VectaShield™ with or without DAPI as appropriate and imaging was performed using a Leica SP5 confocal. Images were edited using ImageJ and Adobe Photoshop 7.0.

Western Blot analysis

Pupal retina were dissected at 40% APF. For each genotype 10 retina were snap-frozen in PBS and SDS sample buffer was added to a final volume of 20μL. Samples were analyzed by Western Blot. Guinea pig anti-Mbt (Walther et al., 2016) and mouse anti-αTubulin (AA4.3, DSHB) (Walsh, 1984) were used for protein detection at concentrations of 1:1000 and 1:200 respectively.

Data analysis

For length and pixel intensity measurements, a threshold was applied to define the *ZA* domain and a line was drawn along the apical-basal axis of the cell, running in the middle of the *ZA* to measure the length of the Arm, Baz, Mbt domains. Mean pixel intensity was measured using the wand (tracing) tool in Fiji (Schindelin et al., 2012). In all cases, at least four independent mosaic retinas were used for each genotype. The intensity profiles of Rap1::GFP, dzy::GFP and Cno relative to Arm were measured in Fiji. A 1μm line was drawn along the apical membrane and continued with a 4μm along the stalk membrane and *ZA*. For each profile, pixel intensities were subjected to unity-based normalization and adjusted such that the normalized maximum value of Arm was placed at 2μm. Statistical analysis was done using Prism 7.0. Data sets were tested for normality (D'Agostino and Pearson normality test) and p-values were calculated using the student's t-test or the Mann-Whitney test as appropriate.

Fluorescence recovery after photobleaching (FRAP)

FRAP analysis was performed as previously described (Walther et al., 2016). At 40% APF the pupal cuticle was removed to expose the retina and the animal was mounted in Voltalef oil. Live imaging was performed on a Leica SP5 confocal using a 63x 1.4 NA oil immersion objective at the following settings: pixel resolution 512 x 512, speed 400 Hz, 10% 488 nm laser power at 20% argon laser intensity and 5x zoom. FRAP analysis of ubi-ECad::GFP

was performed by marking the basal tip of the *AJ* with a 5 pixel-diameter circle ROI followed by photo-bleaching with a single pulse using 90 % 488 nm laser power at 20 % argon laser intensity. *AJ* recovery was recorded every 1.293 seconds with the previously mentioned settings for approximately 1000 sec. FRAP data were drift corrected in Fiji (Schindelin et al., 2012) using the StackReg plugin. Three different Z axis profiles were analyzed: (1) from the photo-bleached area; (2) from an equivalent area of a neighboring non-photo-bleached *AJ*; and (3) from an equivalent area of background. The data were normalized using easyFRAP. ECad::GFP data were fitted to a two-phase association curve in GraphPad Prism. The p values were calculated with an unpaired two-tailed Student's t test with Welch's correction.

Scanning Electron Microscopy

Flies were fixed in 2% paraformaldehyde, 2% glutaraldehyde and 0.1 M cacodylate for 2 hours and then dehydrated in ethanol, as previously described (Richardson and Pichaud, 2010). The samples were then critical-point dried and mounted on aluminum stubs before gold coating. Imaging was carried out on a JEOL Variable Pressure scanning electron microscope (SEM).

REFERENCES

Aaku-Saraste, E., Hellwig, A. and Huttner, W. B. (1996). Loss of occludin and functional tight junctions, but not ZO-1, during neural tube closure--remodeling of the neuroepithelium prior to neurogenesis. *Dev Biol* **180**, 664-79.

Afonso, C. and Henrique, D. (2006). PAR3 acts as a molecular organizer to define the apical domain of chick neuroepithelial cells. *J Cell Sci* **119**, 4293-304.

Berger, S., Bulgakova, N. A., Grawe, F., Johnson, K. and Knust, E. (2007). Unraveling the genetic complexity of Drosophila stardust during photoreceptor morphogenesis and prevention of light-induced degeneration. *Genetics* **176**, 2189-200.

Boettner, B., Harjes, P., Ishimaru, S., Heke, M., Fan, H. Q., Qin, Y., Van Aelst, L. and Gaul, U. (2003). The AF-6 homolog canoe acts as a Rap1 effector during dorsal closure of the Drosophila embryo. *Genetics* **165**, 159-69.

Boettner, B. and Van Aelst, L. (2007). The Rap GTPase activator Drosophila PDZ-GEF regulates cell shape in epithelial migration and morphogenesis. *Mol Cell Biol* **27**, 7966-80.

Bonello, T. T., Perez-Vale, K. Z., Sumigray, K. D. and Peifer, M. (2018). Rap1 acts via multiple mechanisms to position Canoe and adherens junctions and mediate apical-basal polarity establishment. *Development* **145**.

Bos, J. L., de Rooij, J. and Reedquist, K. A. (2001). Rap1 signalling: adhering to new models. *Nat Rev Mol Cell Biol* **2**, 369-77.

Bosch, J. A., Tran, N. H. and Hariharan, I. K. (2015). CoinFLP: a system for efficient mosaic screening and for visualizing clonal boundaries in Drosophila. *Development* **142**, 597-606.

Choi, W., Harris, N. J., Sumigray, K. D. and Peifer, M. (2013). Rap1 and Canoe/afadin are essential for establishment of apical-basal polarity in the Drosophila embryo. *Mol Biol Cell* **24**, 945-63.

de Rooij, J., Boenink, N. M., van Triest, M., Cool, R. H., Wittinghofer, A. and Bos, J. L. (1999). PDZ-GEF1, a guanine nucleotide exchange factor specific for Rap1 and Rap2. *J Biol Chem* **274**, 38125-30.

Freeman, M. (1996). Reiterative use of the EGF receptor triggers differentiation of all cell types in the Drosophila eye. *Cell* **87**, 651-60.

Hayashi, S., Ito, K., Sado, Y., Taniguchi, M., Akimoto, A., Takeuchi, H., Aigaki, T., Matsuzaki, F., Nakagoshi, H., Tanimura, T. et al. (2002). GETDB, a database compiling expression patterns and molecular locations of a collection of Gal4 enhancer traps. *Genesis* **34**, 58-61.

Hogan, C., Serpente, N., Cogram, P., Hosking, C. R., Bialucha, C. U., Feller, S. M., Braga, V. M., Birchmeier, W. and Fujita, Y. (2004). Rap1 regulates the formation of E-cadherin-based cell-cell contacts. *Mol Cell Biol* **24**, 6690-700.

Hong, Y., Ackerman, L., Jan, L. Y. and Jan, Y. N. (2003). Distinct roles of Bazooka and Stardust in the specification of Drosophila photoreceptor membrane architecture. *Proc Natl Acad Sci U S A* **100**, 12712-7.

Huelsmann, S., Hepper, C., Marchese, D., Knoll, C. and Reuter, R. (2006). The PDZ-GEF dizzy regulates cell shape of migrating macrophages via Rap1 and integrins in the Drosophila embryo. *Development* **133**, 2915-24.

Izaddoost, S., Nam, S. C., Bhat, M. A., Bellen, H. J. and Choi, K. W. (2002). Drosophila Crumbs is a positional cue in photoreceptor adherens junctions and rhabdomeres. *Nature* **416**, 178-83.

Jin, D., Durgan, J. and Hall, A. (2015). Functional cross-talk between Cdc42 and two downstream targets, Par6B and PAK4. *Biochem J* **467**, 293-302.

Kawajiri, A., Itoh, N., Fukata, M., Nakagawa, M., Yamaga, M., Iwamatsu, A. and Kaibuchi, K. (2000). Identification of a novel beta-catenin-interacting protein. *Biochem Biophys Res Commun* **273**, 712-7.

Knox, A. L. and Brown, N. H. (2002). Rap1 GTPase regulation of adherens junction positioning and cell adhesion. *Science* **295**, 1285-8.

Krahn, M. P., Buckers, J., Kastrup, L. and Wodarz, A. (2010). Formation of a Bazooka-Stardust complex is essential for plasma membrane polarity in epithelia. *J Cell Biol* **190**, 751-60.

Law, S. H. and Sargent, T. D. (2014). The serine-threonine protein kinase PAK4 is dispensable in zebrafish: identification of a morpholino-generated pseudophenotype. *PLoS One* **9**, e100268.

Mandai, K., Rikitake, Y., Shimono, Y. and Takai, Y. (2013). Afadin/AF-6 and canoe: roles in cell adhesion and beyond. *Prog Mol Biol Transl Sci* **116**, 433-54.

Matsuo, T., Takahashi, K., Kondo, S., Kaibuchi, K. and Yamamoto, D. (1997). Regulation of cone cell formation by Canoe and Ras in the developing Drosophila eye. *Development* **124**, 2671-80.

McGill, M. A., McKinley, R. F. and Harris, T. J. (2009). Independent cadherin-catenin and Bazooka clusters interact to assemble adherens junctions. *J Cell Biol* **185**, 787-96.

Menzel, N., Melzer, J., Waschke, J., Lenz, C., Wecklein, H., Lochnit, G., Drenckhahn, D. and Raabe, T. (2008). The Drosophila p21-activated kinase Mbt modulates DE-cadherin-mediated cell adhesion by phosphorylation of Armadillo. *Biochem J* **416**, 231-41.

Menzel, N., Schneeberger, D. and Raabe, T. (2007). The Drosophila p21 activated kinase Mbt regulates the actin cytoskeleton and adherens junctions to control photoreceptor cell morphogenesis. *Mech Dev* **124**, 78-90.

Morais-de-Sa, E., Mirouse, V. and St Johnston, D. (2010). aPKC phosphorylation of Bazooka defines the apical/lateral border in Drosophila epithelial cells. *Cell* **141**, 509-23.

Nagai-Tamai, Y., Mizuno, K., Hirose, T., Suzuki, A. and Ohno, S. (2002). Regulated protein-protein interaction between aPKC and PAR-3 plays an essential role in the polarization of epithelial cells. *Genes Cells* **7**, 1161-71.

Nam, S. C. and Choi, K. W. (2003). Interaction of Par-6 and Crumbs complexes is essential for photoreceptor morphogenesis in Drosophila. *Development* **130**, 4363-72.

Newsome, T. P., Asling, B. and Dickson, B. J. (2000). Analysis of Drosophila photoreceptor axon guidance in eye-specific mosaics. *Development* **127**, 851-60.

Niessen, C. M. and Gottardi, C. J. (2008). Molecular components of the adherens junction. *Biochim Biophys Acta* **1778**, 562-71.

Nusslein-Volhard, C., Frohnhofer, H. G. and Lehmann, R. (1987). Determination of anteroposterior polarity in Drosophila. *Science* **238**, 1675-81.

O'Keefe, D. D., Gonzalez-Nino, E., Burnett, M., Dylla, L., Lambeth, S. M., Licon, E., Amesoli, C., Edgar, B. A. and Curtiss, J. (2009). Rap1 maintains adhesion between cells to affect Egfr signaling and planar cell polarity in Drosophila. *Dev Biol* **333**, 143-60.

Oda, H. and Tsukita, S. (2001). Real-time imaging of cell-cell adherens junctions reveals that Drosophila mesoderm invagination begins with two phases of apical constriction of cells. *J Cell Sci* **114**, 493-501.

Pannekoek, W. J., Kooistra, M. R., Zwartkruis, F. J. and Bos, J. L. (2009). Cell-cell junction formation: the role of Rap1 and Rap1 guanine nucleotide exchange factors. *Biochim Biophys Acta* **1788**, 790-6.

Pellikka, M., Tanentzapf, G., Pinto, M., Smith, C., McGlade, C. J., Ready, D. F. and Tepass, U. (2002). Crumbs, the Drosophila homologue of human CRB1/RP12, is essential for photoreceptor morphogenesis. *Nature* **416**, 143-9.

Ready, D. F. (2002). Drosophila compound eye morphogenesis: Blind mechanical engineers? In *Results and Problems in Cell Differentiation*, vol. Drosphila Eye Development (ed. K. Moses), pp. 191-204. Berlin Heildelderg New York: Springer-Verlag.

Richard, M., Grawe, F. and Knust, E. (2006). DPATJ plays a role in retinal morphogenesis and protects against light-dependent degeneration of photoreceptor cells in the Drosophila eye. *Dev Dyn* **235**, 895-907.

Richardson, E. C. and Pichaud, F. (2010). Crumbs is required to achieve proper organ size control during Drosophila head development. *Development* **137**, 641-50.

Sawyer, J. K., Harris, N. J., Slep, K. C., Gaul, U. and Peifer, M. (2009). The Drosophila afadin homologue Canoe regulates linkage of the actin cytoskeleton to adherens junctions during apical constriction. *J Cell Biol* **186**, 57-73.

Schindelin, J., Arganda-Carreras, I., Frise, E., Kaynig, V., Longair, M., Pietzsch, T., Preibisch, S., Rueden, C., Saalfeld, S., Schmid, B. et al. (2012). Fiji: an open-source platform for biological-image analysis https://sites.google.com/site/qingzongtseng/imagejplugins. *Nat Methods* **9**, 676-82.

Schmidt, A., Lv, Z. and Grosshans, J. (2018). ELMO and Sponge specify subapical restriction of Canoe and formation of the subapical domain in early Drosophila embryos. *Development* **145**.

Schneeberger, D. and Raabe, T. (2003). Mbt, a Drosophila PAK protein, combines with Cdc42 to regulate photoreceptor cell morphogenesis. *Development* **130**, 427-37.

Spahn, P., Ott, A. and Reuter, R. (2012). The PDZ-GEF protein Dizzy regulates the establishment of adherens junctions required for ventral furrow formation in Drosophila. *J Cell Sci* **125**, 3801-12.

Tepass, U. (2012). The apical polarity protein network in Drosophila epithelial cells: regulation of polarity, junctions, morphogenesis, cell growth, and survival. *Annu Rev Cell Dev Biol* **28**, 655-85.

Wallace, S. W., Durgan, J., Jin, D. and Hall, A. (2010). Cdc42 regulates apical junction formation in human bronchial epithelial cells through PAK4 and Par6B. *Mol Biol Cell* **21**, 2996-3006.

Walsh, C. (1984). Synthesis and assembly of the cytoskeleton of Naegleria gruberi flagellates. *J Cell Biol* **98**, 449-56.

Walther, R. F., Nunes de Almeida, F., Vlassaks, E., Burden, J. J. and Pichaud, F. (2016). Pak4 Is Required during Epithelial Polarity Remodeling through Regulating AJ Stability and Bazooka Retention at the ZA. *Cell Rep* **15**, 45-53.

Walther, R. F. and Pichaud, F. (2006). Immunofluorescent staining and imaging of the pupal and adult Drosophila visual system. *Nat Protoc* **1**, 2635-42.

Walther, R. F. and Pichaud, F. (2010). Crumbs/DaPKC-dependent apical exclusion of Bazooka promotes photoreceptor polarity remodeling. *Curr Biol* **20**, 1065-74.

Wang, Y. C., Khan, Z. and Wieschaus, E. F. (2013). Distinct Rap1 activity states control the extent of epithelial invagination via alpha-catenin. *Dev Cell* **25**, 299-309.

Wei, S. Y., Escudero, L. M., Yu, F., Chang, L. H., Chen, L. Y., Ho, Y. H., Lin, C. M., Chou, C. S., Chia, W., Modolell, J. et al. (2005). Echinoid is a component of adherens junctions that cooperates with DE-Cadherin to mediate cell adhesion. *Dev Cell* **8**, 493-504.

Xu, T. and Rubin, G. M. (1993). Analysis of genetic mosaics in developing and adult Drosophila tissues. *Development* **117**, 1223-37.
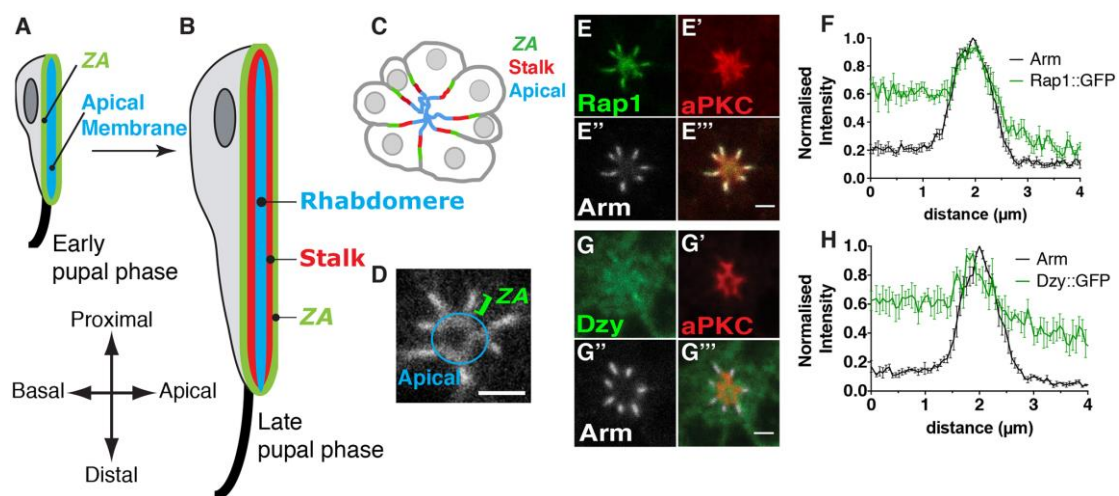
Figures

Figure 1: Dizzy and Rap1 are *ZA* associated proteins. (A-B) Schematic representation of the developing pupal photoreceptor. (A) Early and (B) late stage pupal photoreceptors shown along the lens (top) to brain (bottom) axis of the retina. The apical membrane, which is clearly differentiated by mid pupation and by late pupation forms the rhabdomere, is depicted in blue. The stalk membranes are depicted in red and the *ZA* in green. The axon is depicted as a black line, at the bottom (brain/distal pole) of the cell. (C) Cross section of a cluster (ommatidium) of photoreceptors at mid pupation when the *ZA* (green), stalk membrane (red) and apical membrane (blue) have been specified. (D) Annotated magnification of the Rap1::GFP staining showing the apical membrane and the *ZA*. (E-E''') Photoreceptors expressing Rap1::GFP

(E), stained for aPKC (E') and Arm (E''). Scale bar = 2μm. (F) Intensity profiles of Rap1::GFP and Arm measured along the apical-basal axis. (G-G''') Photoreceptors expressing Dzy::GFP (G), stained for aPKC (G') and Arm (G'') Scale bar = 1.5μm. (H) Intensity profiles of Dzy::GFP and Arm measured along the apical-basal axis.
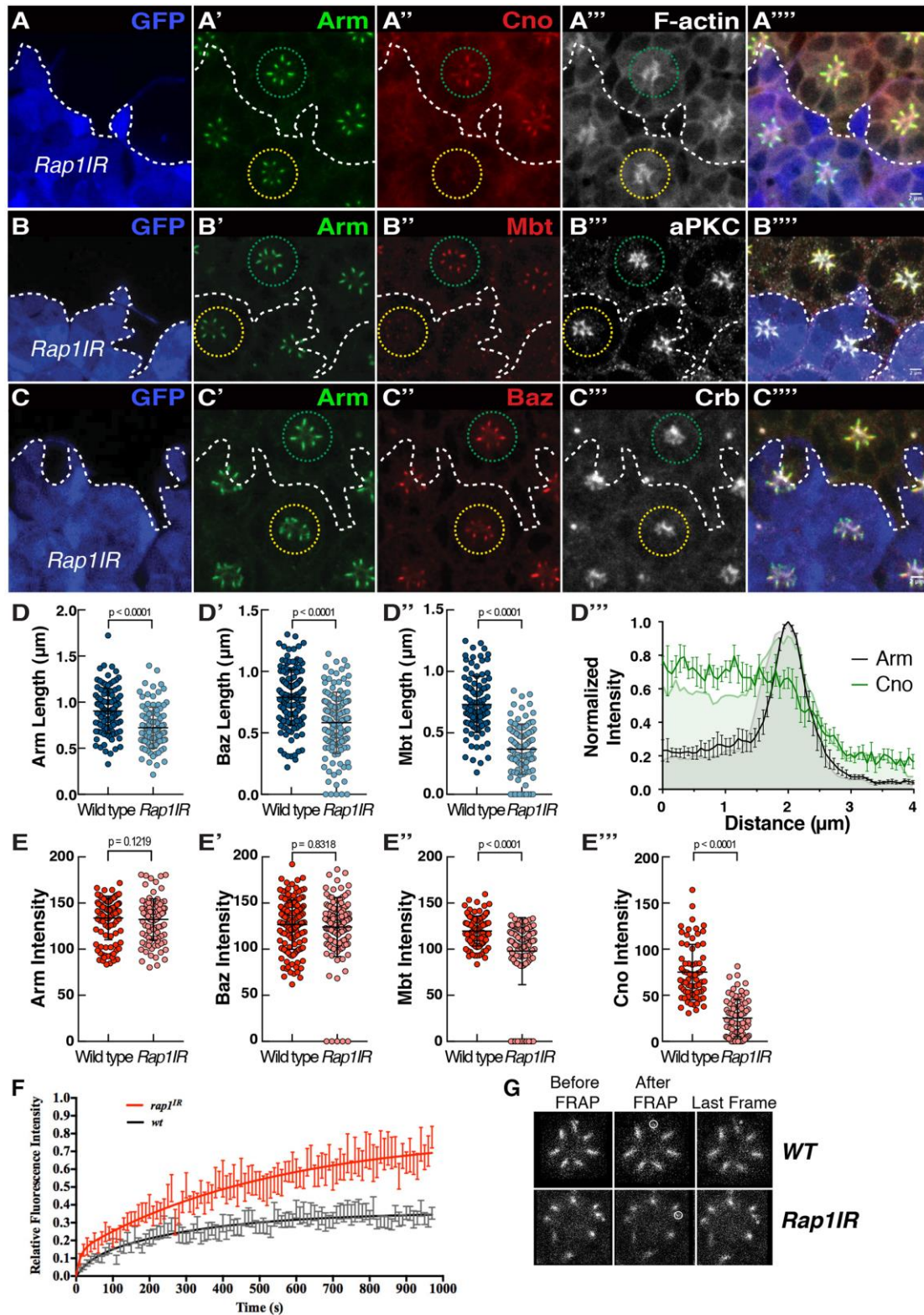
Figure 2: Rap1 regulates the accumulation of *AJ* material during *ZA* morphogenesis. (A-C) *Rap1IR* cells positively labeled by GFP (blue) and stained for Arm (A', B', C'), Cno (A''), Mbt (B''), Baz (C''), F-actin (A'''), aPKC

(B''') and Crb (C''''). Scale bar = 2 μm. (D-D'') Quantification of Arm (D), Mbt (D'), Baz (D'') domain length at the *ZA*. (D''') Normalized intensity profiles of Cno (green) and Arm (grey) in WT photoreceptors (shaded profiles) and *Rap1IR* photoreceptors. (E-E''') Quantification of Arm (E), Mbt (E'), Baz (E'') and Cno (E''') mean pixel intensity at the *ZA*. (F) FRAP fit for E-Cad::GFP in wild type (black) and *Rap1IR* (red) photoreceptors. For both genotypes, the basal end of the developing *ZA* (dashed circle) was photo-bleached (G). For wild type *ZA* FRAP, n = 14 and for *Rap1IR,* n = 12.
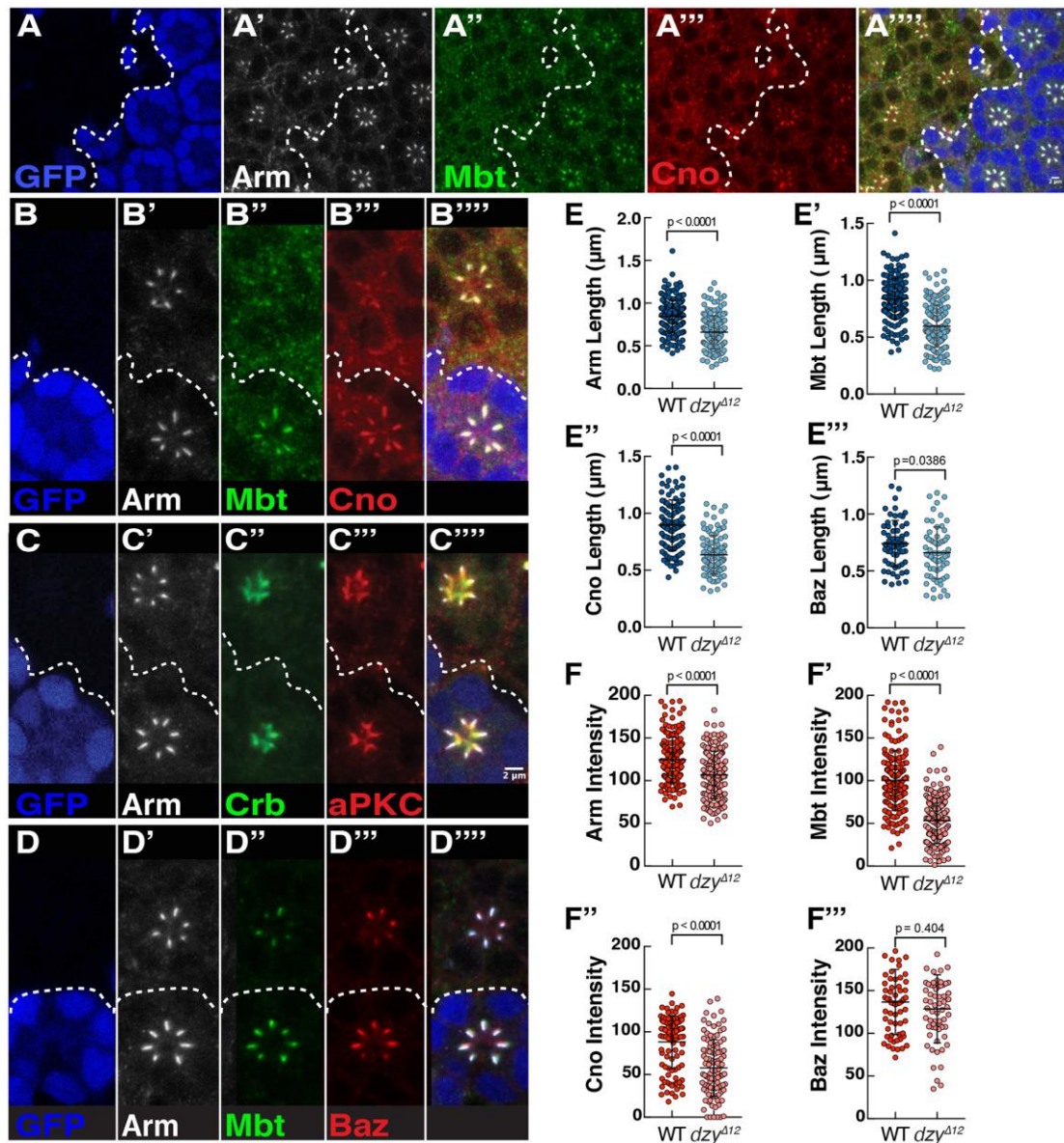
Figure 3: Dzy regulates Cno and Mbt accumulation at the ZA. (A-A''') $dzy^{\Delta12}$ mutant clone labeled by the lack of nuclear GFP (blue), stained for Arm (A'), Mbt (A'') and Cno (A'''). A dashed line highlights the contour of the $dzy^{\Delta12}$ mutant clone. (B-B'''') An ommatidium mutant for dzy (lacking GFP, blue, (B)), (B), stained for Arm (B'), Mbt, (B'') and Cno (B'''). (C-C'''') Ommatidium mutant for dzy (lacking GFP, blue, (C)), stained for Arm (C'), Crb (C'') and aPKC (C'''). (D-D'''') Ommatidium mutant for dzy (lacking GFP, blue, (D)), stained for Arm (D'), Mbt (D'') and Baz (D'''). Scale bars = 2μm. (E-E''') Quantification

of Arm (E), Mbt (E'), Cno (E'') and Baz (E''') domain length at the *ZA*. (F-F''') Quantification of Arm (F), Mbt (F'), Cno (F'') and Baz (F''') mean pixel intensity at the *ZA*.
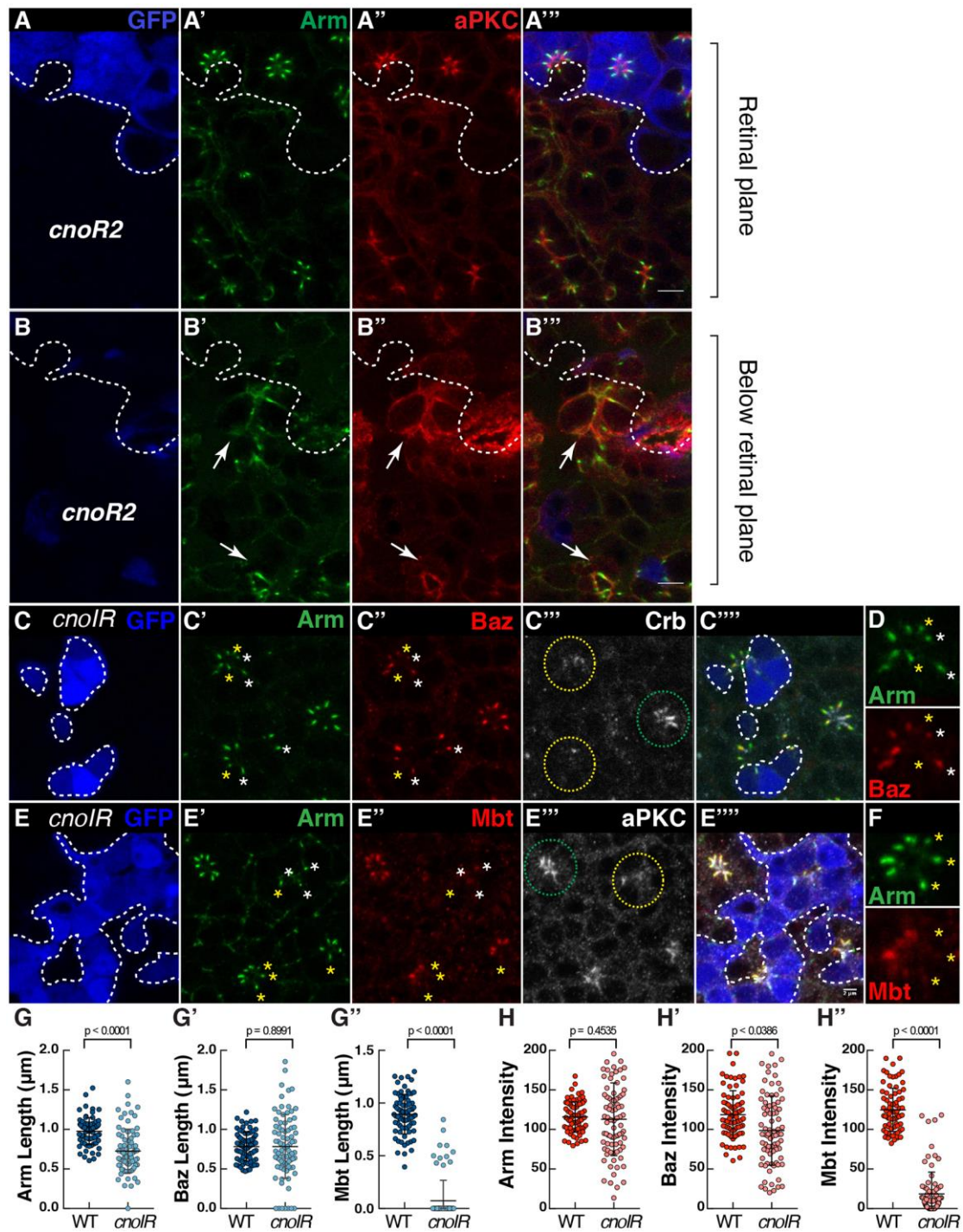
Figure 4: Cno regulates the coupling of Arm, Baz and Mbt at the developing ZA. (A-B) *cno^R2* mutant cells (lacking GFP, blue, (A and B)) stained for Arm (A' and B') and aPKC (A'' and B''). White arrows indicate *cno^R2* mutant photoreceptors that have delaminated from the retinal

neuroepithelium. (C-F) *cnoIR* clones positively labeled by GFP (blue, C and E) and stained for Arm (C' and E'), Baz (C''), Crb (C'''), Mbt (E'') and aPKC (E'''). (D and F) show a magnification of one mosaic ommatidium to highlight the absence of Baz (D) or Mbt (F) in some of the Arm domains. White stars label *ZA* containing both Arm and Baz, while yellow stars indicate *ZA* containing Arm but depleted for Baz (D) or containing Arm but depleted for Mbt (F). Scale bars = 2 μm. (G-G'') Quantification of Arm (G), Baz (G') and Mbt (G'') domain length at the *ZA*. (H-H'') Quantification of Arm (H), Baz (H') and Mbt (H'') mean pixel intensity at the *ZA*.
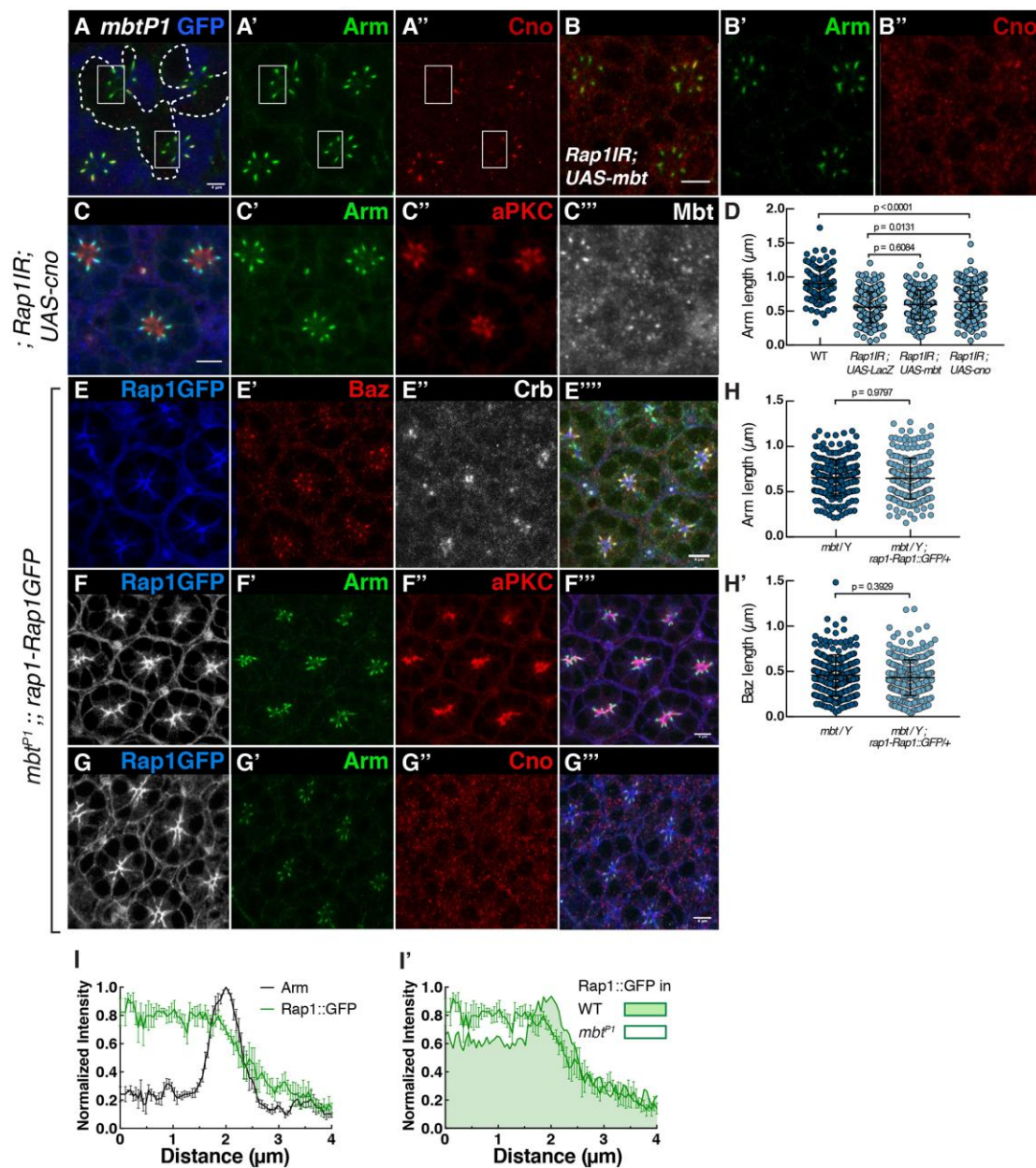
Figure 5: Mbt is required for the accumulation of Cno and enrichment of Rap1 at the *ZA*. (A) *mbt^P1^* mutant photoreceptors (lacking GFP, blue, (A)) and stained for Arm (A') and Cno (A''). White boxes highlight *ZA* within the *mbt^P1^* mutant tissue. (B) *Rap1IR* photoreceptors expressing Mbt and stained for Arm (B') and Cno (B''). (C) *Rap1IR* photoreceptors expressing Cno and labeled for Arm (C'), aPKC (C'') and Mbt (C'''). (D) Quantification of Arm domain length at the *ZA* in wild type photoreceptors, and *Rap1IR*

photoreceptors co-expressing *UAS-LacZ, UAS-mbt* or *UAS-cno*. (E-G) *mbt^{P1}*

mutant photoreceptors expressing *rap1-Rap1::GFP* (E, F, G) stained for Baz

(E'), Arm (F', G'), Crb (E''), aPKC (F'') and Cno (G''). (H) Quantification of the

length of the Arm (H) and Baz (H') domains at the *ZA* in *mbt^{P1}* mutant and

mbt^{P1} mutant expressing *rap1-Rap1::GFP.* (I) Intensity profiles measured for

Rap1::GFP and Arm along the apical-basal axis in *mbt^{P1}* photoreceptors. (I')

Comparison of intensity profiles of Rap1::GFP measured in *mbt^{P1}*

photoreceptors compared to that of wild type photoreceptors (shaded). Scale

bars = 2 μ m.
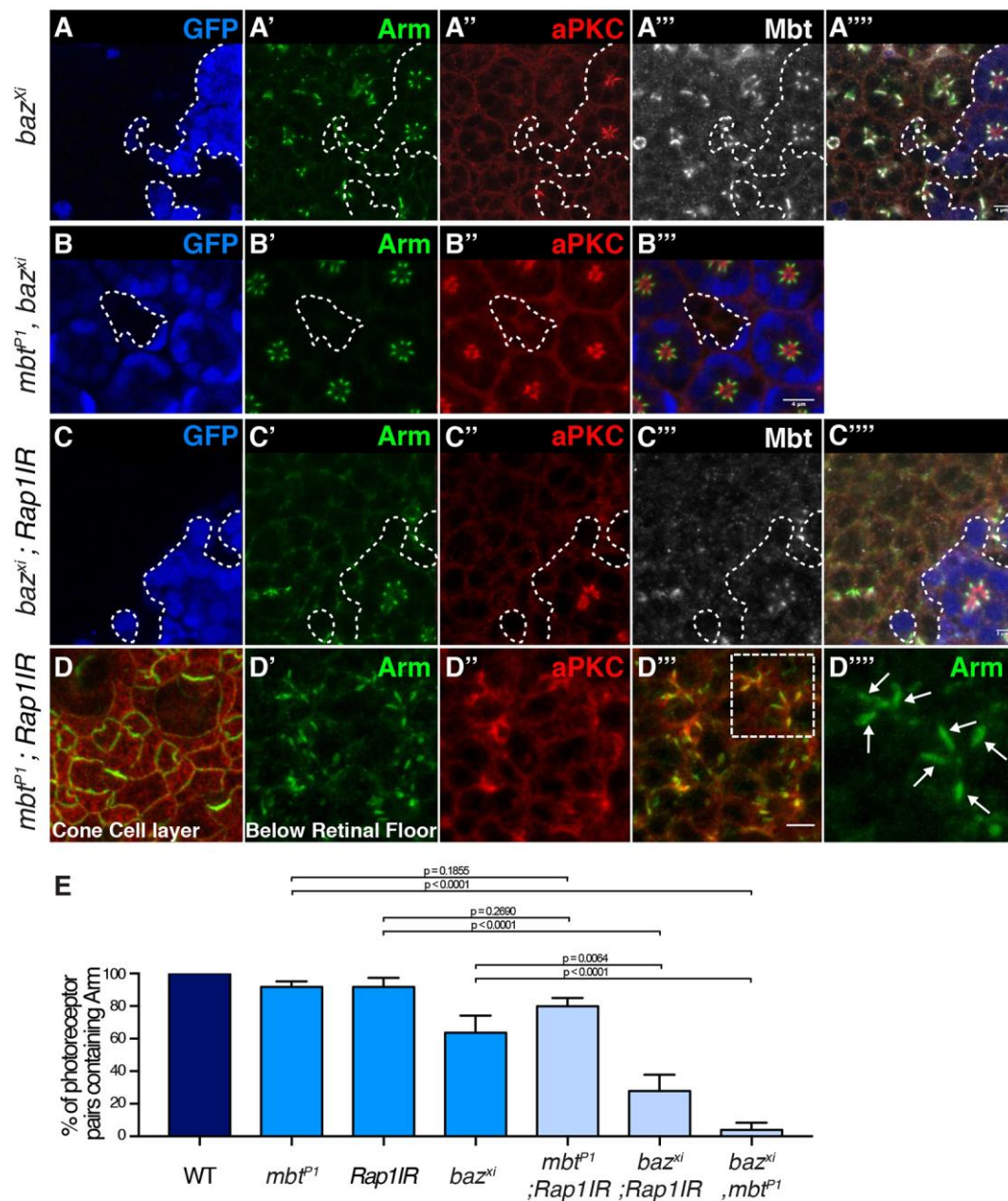
Figure 6: Rap1/Cno and Mbt synergize with Baz to promote *AJ* accumulation at the plasma membrane. (A-A'''') *baz^{xi106}* mutant cells (lacking GFP, blue, (A)) and stained for Arm (A'), aPKC (A'') and Mbt (A'''). (B-B''') *mbt^{P1}*, *baz^{xi106}* double mutant cells (lacking GFP, blue, (B)) and stained for Arm (B') and aPKC (B''). (C-C'''') *baz^{xi106}*, *Rap1IR* double mutant cells (lacking GFP, blue, (C)) and stained for Arm (C'), aPKC (C'') and Mbt (C'''). (D) Confocal section of the cone and pigment cells in an *mbt^{P1}; Rap1IR* retina

stained for Arm (green) and aPKC (red). (D'-D'''') View of the delaminated photoreceptor proximal to (D). (D') Arm, (D'') aPKC, (D''') Merge (D''-D'''); a white-dashed rectangle highlights 2 ommatidia that are magnified in (D''''). White arrows point to *ZA* domains between flanking photoreceptors. (E) Quantification of the percentage of pairs of photoreceptors sharing a lateral Arm domain in wild type, *mbt*[P1]*, Rap1IR, baz*[xi106]*,* double *mbt*[P1]*; Rap1IR,* double *baz*[xi106]*; Rap1IR* and double *baz*[xi106]*, mbt*[P1]*.* Scale bars = 4 μ m.
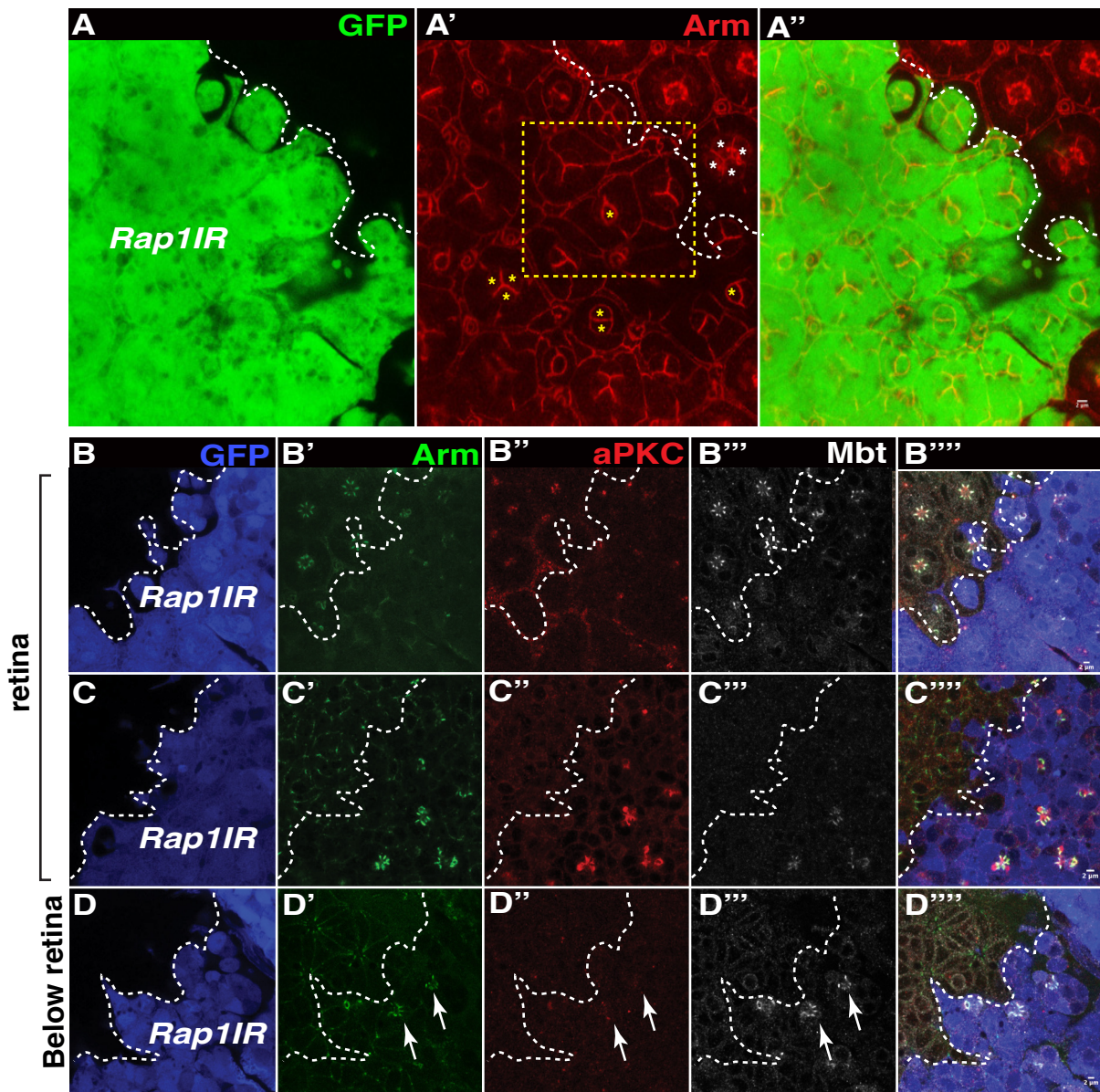
Supplementary Figure 1: Rap1 is required to preserve retinal tissue integrity. (A-A'') *Rap1IR* cells positively labeled by GFP (A) and stained for Arm (A'). Yellow stars label cone cells in the *Rap1IR* tissue. White stars label cone cells in one wild type ommatidium. Note the *Rap1IR* ommatidia lack cone cells. A yellow dashed box highlights *Rap1IR* ommatidia lacking interommatidial cells. (B-D) *Rap1IR* cells positively labeled by GFP (blue, (B, C and D)) and stained for Arm (B', C', D'), aPKC (B'', C'', D'') and Mbt (B''', C''', D'''). Note that many *Rap1IR* photoreceptors delaminate below the floor of the retina, indicated by white arrows (D-D''''). Scale bars = 2μm.

WT   Rap1IR   dzyΔ12/+   Rap1IR ; dzyΔ12/+   bazIR   Rap1IR ; bazIR
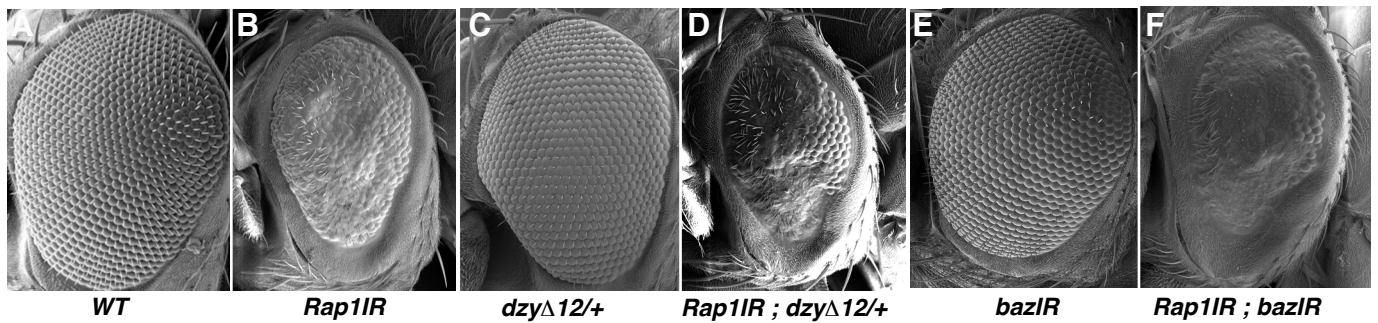
Supplementary Figure 2: Genetic modifiers of the *Rap1IR* rough eye phenotype. (A) SEM of a wild type eye, (B) *Rap1IR*, (C) Heterozygous *dzy*$^{\Delta 12}$ eye, (D) *Rap1IR* combined with *dzy*$^{\Delta 12}$ / +, (E) *bazIR*, (F) *bazIR* combined with *Rap1IR.*
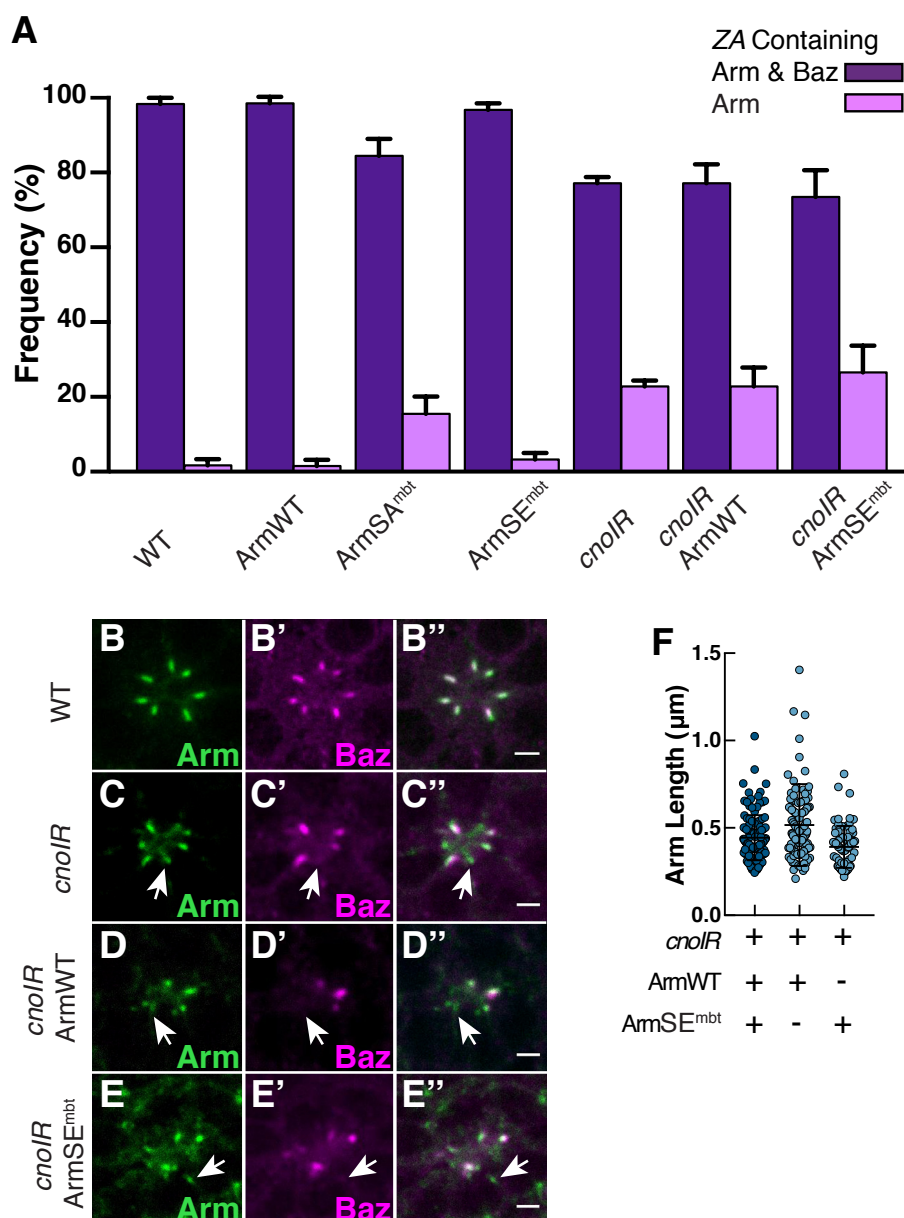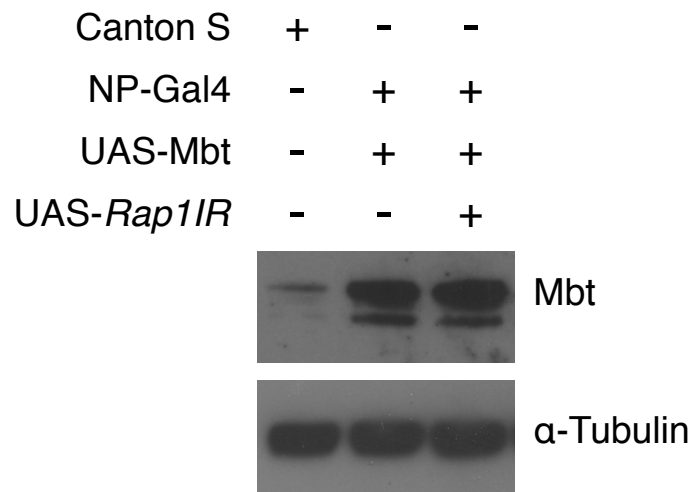
Supplementary Figure 3: Expression of ArmSE^mbt fails to rescue junction length and Baz retention in *cnoIR* photoreceptors

(A) Quantification of the percentage of photoreceptor *ZA* that contain both Arm and Baz (dark purple) or containing Arm but depleted for Baz (light purple). (B-E'') WT (B-B''), *cnoIR* (C-C''), *cnoIR* co-expressing ArmWT (D-D'') or *cnoIR* co-expressing ArmSE^mbt (E-E'') retina, stained for Arm (B, C, D, E) and Baz (B', C', D' and E'). White arrows indicate *ZA* that contain Arm but are depleted for Baz. Scale bars = 2µm. (F) Quantification of Arm domain length at the *ZA* in *cnoIR* photoreceptors and *cnoIR* photoreceptors expressing ArmWT or ArmSE^mbt.
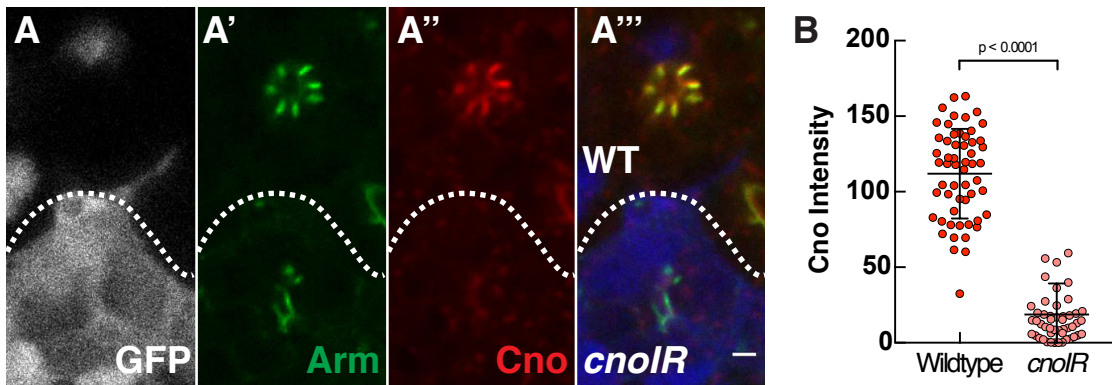
Supplementary Figure 4: *cnoIR* abolishes Cno expression

(A-A''') *cnoIR* cells positively labeled by GFP (A) and stained for Arm (A') and Cno (A''). Scale bars = 2µm. (B) Quantification of residual Cno intensity within the *ZA,* measured along the Arm domain, in *cnoIR* photoreceptors.

Canton S	+	-	-
NP-Gal4	-	+	+
UAS-Mbt	-	+	+
UAS-*Rap1IR*	-	-	+

Mbt

α-Tubulin

Supplementary Figure 5: Expression levels of Mbt in *Rap1IR* retinas

Western blot performed on retinal protein extracts, dissected at 40% after puparium formation.
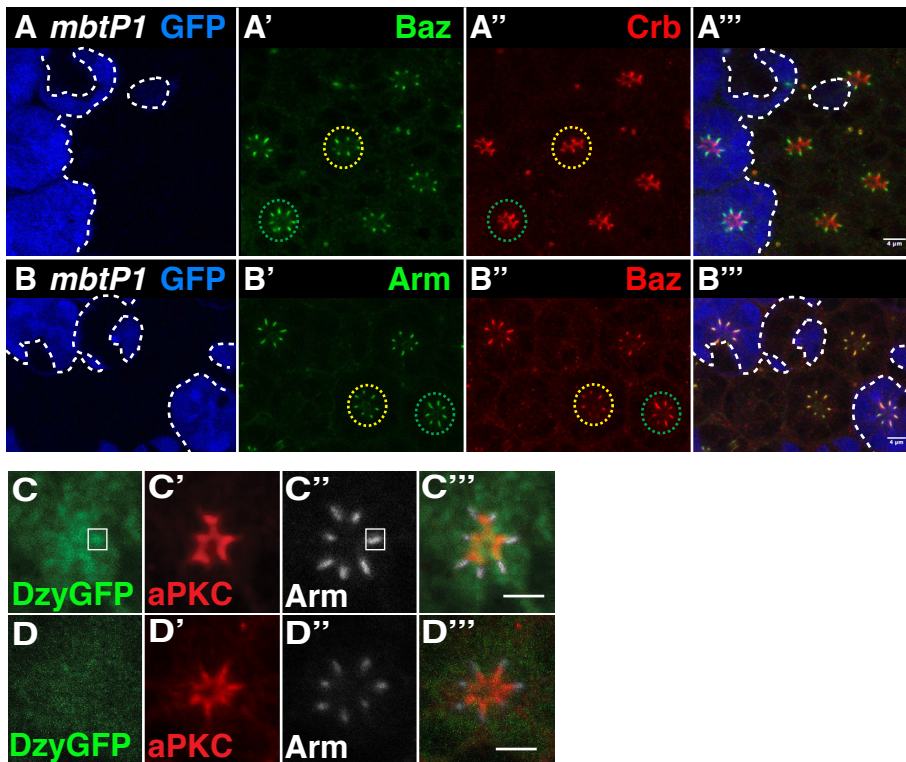
Supplementary Figure 6: Mbt Regulates the accumulation of Arm, Baz and Dzy at the _ZA_. (A-B) *mbt*^{P1} mutant cells (lacking of GFP, blue, (A and B)), stained for Baz (A' and B''), Arm (B') and Crb (A''). (C-C''') Dzy::GFP distribution in wild type photoreceptors (C), stained for aPKC (C') and Arm (C''). (D-D''') Dzy::GFP distribution in *mbt*^{P1} mutant photoreceptors (D), stained for aPKC (D') and Arm (D''). Scale bars = 2µm.